N88-21516

AN EXPERIMENTAL COMPARISON OF SEVERAL CURRENT VISCOPLASTIC CONSTITUTIVE MODELS AT ELEVATED TEMPERATURE

G.H. James, P.K. Imbrie, P.S. Hill, D.H. Allen, W.E. Haisler
Texas A&M University
College Station, Texas 77843

Four current viscoplastic models are compared experimentally for Inconel 718 at 593° C. This material system responds with apparent negative strain rate sensitivity, undergoes cyclic work softening, and is susceptible to low cycle fatigue. The models used include Bodner's anisotropic model, Krieg, Swearengen, and Rhode's model, Schmidt and Miller's model, and Walker's exponential model. Schmidt and Miller's model and Walker's model correct for negative strain rate sensitivity response. A correction similar to Schmidt's is applied to the models of Bodner and Krieg, et al.

A series of tests has been performed to create a sufficient data base from which to evaluate material constants. A method to evaluate the constants is developed which draws on common assumptions for this type of material, recent advances by other researchers, and iterative techniques. A complex history test, not used in calculating the constants, is then used to compare the predictive capabilities of the models.

The combination of exponentially based inelastic strain rate equations and dynamic recovery is shown to model this material system with the greatest success. The method of constant calculation developed in this work was successfully applied to the complex material response encountered. Backstress measuring tests were found to be invaluable and warrant further development.

INTRODUCTION

This paper experimentally compares four current viscoplastic models for metals at elevated temperature. The primary objective of this work is to uncover the mathematical forms which model reality most successfully and to develop basic understanding of the models. A secondary objective is to develop methods of constant calculation which are systematic and repeatable. A final objective is to develop experimental tests and test software to support viscoplastic modeling.

This research produces many positive results. First, the aspects of each model which need further development are uncovered. Also, the most accurate mathematical forms of the models are determined. Third, basic understanding of the models is generated. Such understanding is necessary for actual engineering application of the models and for expanding the capabilities of the models. Fourth, systematic methods of material parameter evaluation are developed which draw on advances by all the modelers. Systematic constant calculation methods make the models much easier to use by researchers and engineers in the field and advance the technology toward automation and standardization. Finally, experimental techniques and needs are developed or reported which can either lead or support theoretical advances.

MATERIAL CONSIDERATIONS

The material used in this work was Inconel 718 and was provided by NASA Lewis Research Center in Cleveland, Ohio. The temperature used was 593° C. (1100° F.). The average value of Young's modulus was 169.9 GPa. The material used in this work had .2% yield stress values between 792 and 903 MPa. The material cyclically work softened. Strain ageing and negative strain rate sensitivity effects were observed between the strain rates of $1X10^{-5}$ sec^{-1} and $1X10^{-3}$ sec^{-1}. A fatigue life of 5 to 30 cycles resulted when specimens were cycled at strain amplitudes over $\pm$1% strain. Lower strain rates and the inclusion of creep hold times also adversely affected the fatigue life.

All samples were subjected to the same heat treatment prior to testing. The heat treatment used was given by the Metals Handbook [1]. The material was annealed at 954° C for one hour and then oil quenched. The next step was

ageing at 718° C. for eight hours with a furnace cool. The furnace used was a Hevi Duty Electric Co. type 66-P. Temperature was monitored with a Keithly 871 Digital Thermometer. The resulting material state was found to be the easiest to machine. Therefore, the heat treatment was carried out before machining and again before testing.

OVERVIEW OF MODELS

The models chosen for this work include Bodner's anisotropic model [2], Krieg, Swearengen, and Rhode's model [3], Schmidt and Miller's model [4], and Walker's exponential model [2]. These models were chosen because they are under active development, methods of determination of the constants have been reported, and some attempt has been made or is being made to expand them to transient temperature modeling. The material utilized in this work responded with negative strain rate sensitivity due to strain ageing. The models of Schmidt and Miller and Walker were able to handle this phenomenon. The models of Bodner and Krieg, et al. needed corrections to handle this effect. The models are reviewed below.

Bodner's Anisotropic Model

The growth laws for Bodner's anisotropic model have the following form:

$$\dot{\varepsilon}^I = \frac{2}{\sqrt{3}} D_0 \exp\left\{ -\frac{1}{2}\left[\frac{Z}{\sigma}\right]^{2n}\right\} \operatorname{sgn} \sigma \tag{1}$$

$$Z = Z^I + Z^A = Z^I + B \operatorname{sgn} \sigma \tag{2}$$

$$\dot{Z}^I = m_1\left[Z_1 - Z^I\right] \dot{W}_p - A_1 Z_1 \left[\frac{Z^I - Z_2}{Z^1}\right]^{r_1} \tag{3}$$

$$\dot{B} = m_2\left[Z_3 \operatorname{sgn} \sigma - Z^A\right] \dot{W}_p - A_2 Z_1 \left[\frac{|B|}{Z_1}\right]^{r_2} \operatorname{sgn} Z^A \tag{4}$$

where D_0, n, m_1, Z_1, Z_2, A_1, r_1, m_2, Z_3, A_2, and r_2 are material constants.

The flow law is exponentially based as seen in equation (1). The model gives a limiting strain rate in shear of D_0 [5]. The term $-m_1 Z^I \dot{W}_p$ is a dynamic recovery term for Z^A in the isotropic growth law (3) and $-A_1 Z_1\left[\left(Z - Z_2\right) Z_1^{-1}\right]^{r_1}$ is a static thermal recovery term. B is a uniaxial representation of a second order tensor in the multiaxial state which handles directional or anisotropic hardening. B is assumed to act as an

isotropic variable on an incremental basis [6]. The growth law for B (4) has the same components as the growth law for D (3).

Bodner's model is seen to use the rate of plastic work instead of inelastic strain rate as the measure of work hardening (3,4). This is designed to allow for better modelling of strain rate jump tests [7]. The correction used to account for the strain ageing effects was Schmidt and Miller's non-interactive solute strengthening correction [4]. The inelastic strain rate equation was then written in the following form:

$$\dot{\varepsilon}^I = \frac{2}{\sqrt{3}} D_0 \exp\left[-\frac{1}{2}\left(\frac{Z + F_{sol}}{\sigma}\right)^{2n}\right] \operatorname{sgn} \sigma \tag{5}$$

$$F_{sol} = F \exp\left\{-\left[\frac{\log(|\dot{\varepsilon}^I|) - \log(J)}{\beta}\right]^2\right\} \tag{6}$$

where F is the maximum correction, J is the strain rate of maximum correction, and β is the width of correction.

Krieg, Swearengen, and Rhode's Model

Krieg, et al.'s growth laws have the following form:

$$\dot{\varepsilon}^I = C\left(\frac{\sigma - B}{D}\right)^n \operatorname{sgn} \sigma \tag{7}$$

$$\dot{B} = A_1\dot{\varepsilon}^I - A_2 B^2\left[\, e^{(A_3 B^2)} - 1 \,\right] \operatorname{sgn} B \tag{8}$$

$$\dot{D} = A_4\dot{\varepsilon}^I - A_5(D - D_0)^n \tag{9}$$

where C, n, A_1, A_2, A_3, A_4, and A_5 are material constants.

The flow law is seen to be a power law based equation. The back stress and drag stress growth laws (8,9) contain static thermal recovery terms but no dynamic recovery terms. The recovery term in (8) is based on a dislocation climb model by Friedel. The recovery term in (9) is based on a special case of the same climb recovery model used in (8) [3,8].

Schmidt and Miller's non-interactive solute strengthening correction was again used with this model to produce the following inelastic strain rate equation:

$$\dot{\varepsilon}^I = C\left(\frac{\sigma - B}{D + F_{sol}}\right) \operatorname{sgn}(\sigma - B) \tag{10}$$

$$F_{sol} = F \exp\{ - [\frac{\log(|\dot{\varepsilon}^I|) - \log(J)}{\beta}]^2\} \quad (11)$$

Schmidt and Miller's Model

Schmidt and Miller's growth laws have the following form:

$$\dot{\varepsilon}^I = B'\{ \sinh(\frac{\sigma - B}{D + F_{sol}})^{1.5}\}^n \operatorname{sgn}(\sigma - B) \quad (12)$$

$$\dot{B} = H_1\dot{\varepsilon}^I - H_1B'\{ \sinh(A_1|B|) \}^n \operatorname{sgn}(B) \quad (13)$$

$$\dot{D} = H_2|\dot{\varepsilon}^I|(C_2 + |B| - \frac{A_2}{A_1} D^3) - H_2C_2B'\{ \sinh(A_2D^3) \}^n \quad (14)$$

$$F_{sol} = F \exp\{ - (\frac{\log(|\dot{\varepsilon}^I|) - \log(J)}{\beta})^2\} \quad (15)$$

where B', n, H_1, A_1, H_2, C_2, A_2, F, J, and β are material constants.

The flow law has the form of a hyperbolic sine. This form was chosen to model creep response better [9]. This same form is found in the static thermal recovery terms of the back stress and drag stress growth laws (13,14). The drag stress hardening term contains a hardening term, a dynamic recovery term, and a term which couples drag stress hardening to back stress magnitude. These three terms provide the proper cyclic, hardening, softening and saturation behavior [9]. The same non-interactive solute strengthening correction (F_{sol}) as mentioned earlier is seen in this model.

Walker's Exponential Model

The growth laws for Walker's exponential model have the following form [2,10]:

$$\dot{\varepsilon}^I = \frac{\exp(\frac{\sigma - B}{D}) - 1}{\beta} \operatorname{sgn}(\sigma - B) \quad (16)$$

$$\dot{B} = n_2 - B\{ [n_3 + n_4\exp(-n_5| \log(\frac{|\dot{R}|}{\dot{R}_0}) |)] \dot{R} + n_6\} \quad (17)$$

$$D = D_1 + D_2\exp(-n_7R) \quad (18)$$

$$\dot{R} = |\dot{\varepsilon}^I| \quad (19)$$

where β, n_2, n_3, n_4, n_5, $\dot{R}_0$, n_6, D_1, D_2, and n_7 are material constants.

This version of Walker's flow law (16) is based on an exponential

function. The term $n_2\dot{\varepsilon}^I$ is seen to be a work hardening term in the back stress growth law. The term $B\left[n_3 + n_4 \exp(-n_5 |\log(|\dot{R}|/\dot{R}_0|)|\right] \dot{R}$ is a dynamic recovery term. Negative strain rate sensitivity effects can be modelled with the term $n_4 \exp(-n_5 |\log(|\dot{R}|/\dot{R}_0)|)$. Back stress thermal recovery is handled by the $B\, n_6$ term. Drag stress hardening is modelled through the $D_2 \exp(-n_7 R)$ term. No provision is made for drag stress recovery in this model.

EXPERIMENTAL PROGRAM

The basic experimental program consisted of the following tests:

(1) 2 monotonic tension tests to 1.5% strain (strain rates of 3.15×10^{-3} sec^{-1} and 7.25×10^{-6} sec^{-1});

(2) 5 fully reversed cyclic tests to $\pm$ .8% strain (strain rates between 1.00×10^{-3} sec^{-1} and 7.63×10^{-6} sec^{-1});

(3) 5 constant load creep tests (applied stresses between 820 MPa and 958 MPa);

(4) 4 back stress measuring tests during cyclic loading and 4 during secondary creep; and

(5) 1 complex history test.

Table 1 provides more specific information on the test program. Column 1 provides the test number. The type of test is given in column 2. The strain rate and strain limits are given in columns 3 and 4. The applied stresses for the creep tests are given in column 5. A complete data set in tabular form is provided in reference [11].

Back Stress Measuring Tests

Back stress measuring tests during secondary creep as described by Krieg, et al. [3] and during saturated cyclic loading as used by Walker [12] were performed in this work. The cyclic back stress numbers were obtained by holding a saturated cyclic test at various points on the unloading curve, switching to load control and monitoring the strain rate following the hold. The material was recycled and a hold time at another stress value was carried out. Fatigue lifetime problems for the material used in this work did not permit complete saturation of the microstructure for fear of sample fracture. The criterion used to define saturation in this work was a cycle to cycle variation of the maximum stress of less than 6.89 mpa. These conditions

Table 1 - Test Program

Test	Type	$\dot{\varepsilon}_{app}$ sec^{-1}	ε_{lim}	σ_{app} MPa
70	tension	3.151E-3	1.5%	
71	tension	7.253E-6	1.5%	
86	cyclic	1.002E-3	+/-.8%	
56	cyclic	9.966E-4	+/-.8%	
65	cyclic	3.127E-4	+/-.8%	
83	cyclic	9.926E-5	+/-.8%	
80	cyclic	3.054E-5	+/-.8%	
72	cyclic	7.626E-6	+/-.8%	
64	creep			956.3
63	creep			922.6
62	creep			875.0
61	creep			854.4
60	creep			819.9
84	back	2.812E-3	+/-.8%	
88	back	9.272E-4	+/-.8%	
81	back	8.635E-4	+/-.8%	
65	back	3.127E-4	+/-.8%	
63	back			922.6
62	back			875.0
61	back			854.4
60	back			819.9
89	complex			

were met after 10 to 15 cycles for this material.

A linear least squares regression to the strain rate data provided a strain rate at each hold time. Each transient test had to be individually scrutinized to decide how many points to consider in the regression analysis as the onset of thermal recovery following a hold time was a very subjective decision. The back stress was assumed to be equal to the hold stress at which a zero strain rate was produced. This hold stress was determined by the use of a linear least squares curve fit to the strain rate versus hold stress data.

The creep back stress numbers were obtained in a similar fashion. The stress on a sample in secondary creep was dropped to various lower levels. The inelastic strain rate immediately following each drop was analyzed in the same manner as with the cyclic tests.

The back stress numbers were invaluable in estimating some material constants. The results were also promising enough to warrant further study. The procedures used here could be greatly enhanced by equipment with greater resolution such as used by Jones, et al. [13] and less subjective methods of

data reduction such as the method of Blum and Finkel [14]. Other techniques such as torsional cycling used by Ellis and Robinson could also be considered [15]. The stress transient test [16] might also provide information for a material such a Inconel 718 which suffers from a short fatigue life when cycled. Reference [11] contains more information on the results observed and software developed for these tests.

EXPERIMENTAL APPARATUS

The load frame utilized in these tests was an MTS (Materials Test System) model 880 electrohydraulic testing machine shown in Fig. 1. MTS 652.01 Water-cooled hydraulic grips allowed fully reversed cyclic tests to be carried out at high temperature. The frame was controlled by a Digital Micro PDP-11 computer. Computer programs were written to run monotonic tension tests, cyclic tests, cyclic tests with hold times, creep tests, and creep stress drop tests. The Micro PDP-11 also handled data acquisition functions. An MTS 661.21A-02 50 KN load cell was the load transducer. An MTS 632.41B-02 axial extensometer was the strain transducer. This device had quartz extension rods which contacted the sample at two 120° punch holes. The material samples designed to ASTM E606-77T specifications for low cycle fatigue specimens.

An MTS 652 three-zone clamshell furnace and three Research Incorporated 63911 Process Temperature and Power Controllers were used for temperature control. Temperature Measurement was handled by six 28 gauge K-type thermocouples. These were placed in contact with the sample. Three thermocouples were fed into a Fluke 2176A Digital Thermometer for readout. These were placed with one each at the top, middle, and bottom of the gauge section. The other three thermocouples were fed into the temperature controllers. These were placed in the center of the furnace zone each was to sense with one thermocouple placed in the center of the gauge section and one on each grip.

The thermocouples were fastened to the grips by fiberglass thread attached to the sample by self-supporting means. The thermocouples at the top and bottom of the gauge section were wound around the sample. The thermocouples used in the center of the gauge section were brought into the oven from different directions and tied to each other. These thermocouples were then wound around the sample for contact. Welding the thermocouples to

the sample would have produced harder contacts with more reliable temperature measurement. However premature failure occurred at the welds.

CALCULATION OF MATERIAL CONSTANTS

The complex response of Inconel 718 at 593° C prompted flexible methods of constant calculation to be developed. The method for calculating constants for the models began by making a series of judicious assumptions which allowed commonly used constant calculation schemes to produce initial estimates of the constants. Some nonlinearity was avoided in this step and was reintroduced by a series of repeatable iterations to the final constants. The iterative step numerically integrated the models to predict the stress-strain response at a certain point. One material constant was then changed to match the prediction to the experimental value at this point. Another material constant was then changed to match another material point.

Physical insight, familiarity with the uncertainty in the data set, and engineering intuition guided the organization of the calculation process. However, the actual process was carried out as systematically as possible. The eventual creation of systematic and automatable methods to calculate constants has been a major driver in this phase of the work. The method used to calculate the material constants will be summarized using a generic viscoplastic model in the first subsection of this section. The generic model used as an example will be presented first followed by a subsection outlining the general method of initial calculations and a subsection outlining the iterative step.

Generic Viscoplastic Model

The growth laws for the example model are presented below:

$$\dot{\varepsilon}^I = \left(\frac{\sigma - B}{D}\right)^n \tag{20}$$

$$\dot{B} = C_1 \dot{\varepsilon}^I + C_2 B \, \dot{\varepsilon}^I + C_3 B \tag{21}$$

$$\dot{D} = C_4 |\dot{\varepsilon}^I| + C_5 D \tag{22}$$

n is a constant measuring strain rate sensitivity. C_1 is a constant measuring back stress hardening. C_2 is handling back stress dynamic recovery and C_3

measures back stress thermal recovery. C_4 produces drag stress hardening and C_5 models drag stress recovery.

Initial Assumptions

The following initial assumptions were made in this work:

(1) back stress was assumed responsible for hardening in monotonic tension;

(2) drag stress was assumed responsible for cyclic softening;

(3) thermal recovery was assumed negligible for rapid tests ($\dot{\varepsilon}^I \geq 1.0X10^{-4} sec^{-1}$) ;

(4) drag stress thermal recovery was present in low strain rate saturated cyclic tests; and

(5) back stress thermal recovery was present in creep tests.

These assumptions allowed the constants for the inelastic strain rate equations, back stress hardening, drag stress hardening, drag stress recovery, and back stress recovery to be calculated in that general order. These assumptions also allowed much of the constant calculation schemes reported in the literature to be utilized with this material [2,3,4,5,9,12,17,18].

The first step was to estimate the constants in the back stress growth law assuming thermal recovery was negligible. The back stress growth law took on the following form:

$$\dot{B} = [C_1 + B\ C_2]\ \dot{\varepsilon}^I \qquad (23)$$

Differential techniques for calculating work hardening such as seen in Chan's gamma and theta plot concepts [2] were useful. Experimental estimations of back stress values such as used by Krieg, et al. [3] and Walker [12] were usually necessary. Relationships between saturated stresses and saturated back stresses as used by Miller [9] have also been used.

The next step was to calculate the strain rate sensitivity constant n and the initial value of drag stress denoted by D_0. Rewriting the inelastic strain rate equation in the following form was useful:

$$\ln(\ \sigma - B\ ) = \frac{1}{n} \ln(\ \dot{\varepsilon}^I) + \ln(\ D_0) \qquad (24)$$

A linear fit to several data points typically provided 1/n as the slope and $\ln(\ D_0\ )$ as the intercept. This is a technique commonly used with Bodner's

model [19]. The ability to estimate saturated stresses and back stresses using techniques such as the gamma or theta plot [2] and relations between saturated stress and back stress are useful [9,2].

Initial determination of the drag stress parameter C_4 was carried out by assuming that thermal recovery could be neglected for rapid tests. The cumulative inelastic strain was calculated at a point on the cyclic curve where B and D could be estimated. The drag stress recovery parameter C_5 was then calculated by assuming the drag stress growth law was equal to zero for the saturated cycle of a low strain rate test. The back stress recovery parameter C_3 was calculated by assuming the growth law for back stess was zero for creep tests.

Computer Iterations

The computer iterations began by pairing each material constant with an experimental stress-strain point which the constant should intuitively have the greatest effect in predicting in a sequential fashion. The constants in the generic model were paired in the following fashion for this work:

(1) D_0 was paired with a stress-strain point at .8% strain on test 70 ($\dot{\varepsilon} = 3.151X10^{-3}$ sec^{-1});

(2) C_2 was paired with a stress-strain point at 1.3% strain on test 70;

(3) C_1 was used to assure that the theoretical back stress values were in the same range expected from experimental values;

(4) n was paired with a stress-strain point at .8% strain on test 71 ($\dot{\varepsilon} = 7.253X10^{-6}$ sec^{-1});

(5) C_3 was paired with a point at 1.3% strain on test 71;

(6) C_4 was paired with a point at .8% on the 10th cycle of test 86 ($\dot{\varepsilon} = 1.002X10^{-3}$ sec^{-1});

(7) C_5 was paired with a point at .8% ot the 4th cycle of test 72 ($\dot{\varepsilon} = 7.626X10^{-6}$ sec^{-1});

The iterative procedure then progressed by numerically integrating the model to predict the experimental stress-strain value for a specific constant. The constant was altered to match this point while the others were held constant. Then another constant was altered to produce the proper prediction at its paired experimental point. The expected order with which these steps were to be carried out is shown in Table 2. The x marks indicate which constant is being altered during the step indicated in column 1. Steps 1 through 5 are setting the back stress hardening characteristics. Steps 6

through 9 are setting the strain rate sensitivity of the model. Steps 10 through 12 are setting the drag stress hardening constant. The back stress recovery constants are being set in steps 13 through 15. Drag stress recovery is set in steps 16 through 18.

Table 2 - An Example Set of Iterations

Step	D_0	C_2	C_1	n	C_4	C_3	C_5
1	x						
2		x					
3			x				
4	x						
5		x					
6				x			
7	x						
8		x					
9				x			
10					x		
11		x					
12					x		
13						x	
14		x					
15						x	
16							x
17						x	
18							x

This method allows the entire process to be recorded. Automation of such a method is also possible if the initial calculations produce values which are close to the final constants. A systematic set of iterations may also allow a standard method for calculating constants to be produced. The lack of correction for strain ageing effects in the initial calculations caused problems in implementing this iterative scheme. Reference [11] provides some suggestions to avoid this as well as the specific application of this method to the models used in this work. Table 3 gives the final values of the constants with stress units of MPa, strain units of cm/cm, and time units of sec.

MODEL RESULTS

The forms of the models to be covered in this section include Bodner's model without a correction for solute strengthening, Bodner's model with a

Table 3 - Final Constants for Models

Krieg, Swearengen and Rhode's Model	
Constant	Final Value
n	15.00
C (1/sec)	2.000E-4
A1 (MPa)	9,646
A2 (1/(MPa sec))	0.000
A3 (MPaE-2)	2.387E-5
A4 (MPa)	-3445
A5 (MPaE(1-n)/sec)	-1.137E-19
D0 (MPa)	689.0
F (MPa)	379.0
β	1,000
J	7.000E-6

Schmidt and Miller's Model	
Constant	Final Value
n	7.0
A1 (1/MPa)	1.451E-4
A2 (MPaE-3)	.030572
B' (1/sec)	1.5E6
C2 (MPa)	-2.067E5
D0 (MPa)	.006890
H1 (MPa)	.4823
H2 (secE(1/n))	1E-7
F (MPa)	.04823
β	3.5
J	1E-9

Bodner's Anisotropic Model	
Constant	Final Value
n	.8132
A1 (1/sec)	-.0010
A2 (1/sec)	0.000
M1 (1/MPa)	.007257
M2 (1/MPa)	.05805
r1	.4926
r2	.4926
Z0 (MPa)	6201
Z1 (MPa)	4823
Z2 (MPa)	6201
Z3 (MPa)	2184
F (MPa)	-2412
β	3.0
J	1.0E-6

Walker's Exponential Model	
Constant	New Value
C	1.000E40
D1 (MPa)	4.823
D2 (MPa)	2.067
n2 (MPa)	2.274E5
n3	750.0
n4	-250.0
n5	.6600
n6	2.5E-4
n7	18.00
R0	3.050E-5

solute strengthening correction, the model of Krieg, et al. with and without a correction for solute strengthening, Schmidt and Miller's model, and Walker's exponential model. The models were numerically integrated with an Euler forward integration scheme on a Perkin-Elmer 32-10 computer. The time steps used ranged from $5.0X10^{-4}$ sec for test 70 to $5.0X10^{-2}$ sec for test 71.

Reproduction of Test Data

Fig. 2 shows the response of the models as compared to test 70 ($\dot{\varepsilon} = 3.151X10^{-3}$ sec^{-1}). The models are all oversquare except for Walker's. Walker's model is showing adverse effects from its dynamic recovery term as the stress is decreasing at higher strain levels. This is more of a problem with the method of constant calculation than the model itself. The iterative portion of the constant calculation process was performed with access to only two points on this curve. Using three points or interactive graphics would have solved this problem.

Fig. 3 compares the model outputs to test 71 ($\dot{\varepsilon} = 7.253X10^{-6}$ sec^{-1}). Walker's model is still following the shape of the curve best. The dynamic recovery problem still exists with the Walker model. The Krieg, et al. model is showing some numerical instability due to the presence of the solute strengthening parameters. The uncorrected versions of Bodner and Krieg, et al. are much lower than the other models. The F_{sol} parameter was simply set to zero in these versions. The other constants remained the same as in the corrected versions. Therefore, the reponse of the uncorrected versions could have been averaged over the strain range better. However, the basic strain rate sensitivity would have remained the same.

Fig. 4 interpolates the model response and experimental response between these two strain rates presented above by picking off stress values at .8% total strain for tests of intermediate strain rates and plotting these values versus the log of the applied strain rate. The tests used in Fig. 2 and Fig. 3 are shown on this figure also. Walker's model is exhibiting negative strain rate sensitivity and the corrected Bodner model is showing no strain rate sensitivity. The other models clearly produce positive strain rate sensitivity.

Fig. 5 shows the stress values at +.8% strain for the saturated cycle response. The slowest strain rate provides data from the fourth cycle and the other points are from the 10th cycle. The trend has changed and all the models with correction for solute strengthening are exhibiting negative strain

rate sensitivity. This is probably an effect of the drag stress thermal recovery parameters and the cyclic work softening response.

Fig. 6 allows interpolation between the first cycle and the 10th cycle of test 86 ($\dot{\varepsilon} = 1.002X10^{-3}$ sec^{-1}) by presenting the values at +.8% strain for each cycle. The corrected Krieg, et al. model and the uncorrected Bodner model reproduce this data closest. Fig. 7 provides the same data for test 80 ($\dot{\varepsilon} = 9.926X10^{-5}$ sec^{-1}). This strain rate shows Walker's model following the experiment the closest. The peak value at the second cycle is reproduced with this model only. Fig. 8 presents the cyclic data for test 72 ($\dot{\varepsilon} = 7.626X10^{-6}$ sec^{-1}). The corrected Bodner model is following the data closest. The Walker model is clearly suffering from the lack of a drag stress thermal recovery term.

Predictive Capabilities

The predictive capabilities of the models were explored by the use a complex history test. This experimental test was not used in the calculation of the material constants. Table 4 gives the input history of this test. Fig. 9 through Fig. 14 show the comparison of the models to this complex history test. The corrected Bodner model in Fig. 10 is the least affected by strain rate jumps. Bodner attributes this to the use of plastic work as the measure of work hardening [7]. The interaction of the solute strengthening corrections of all the models may be having an effect on this aspect of all the models. The uncorrected versions in Fig. 9 and Fig. 11 are very suseptible to these jumps. Yao and Krempl report that the overshoots and undershoots observed during the strain rate jumps are a transient effect of the behavior of a system of coupled nonlinear differential equations [20].

A comparison of the response of the corrected and uncorrected versions of the Bodner and Krieg, et al. models at the zero strain hold time shows that the F_{sol} correction negates the effects of thermal recovery in such instances. This could be a result of the low value of J or the inelastic strain rate of maximum correction used in these models. The corrected Bodner model had $J = 1.0X10^{-6}$ sec^{-1}, the model of Krieg, et al had $J = 7.0X10^{-6}$ sec^{-1}, and Schmidt and Miller had $J = 1.0X10^{-9} sec^{-1}$. Schmidt and Miller's model showed no thermal recovery at this hold either. The small inelastic strain rates produced by thermal recovery terms would meet increasing hardness if their magnitude was below J. Increasing hardness would tend to drive the stresses up and oppose the action of the thermal recovery terms.

Table 4 - Complex History Test Input

Interval	Beginning Strain	Ending Strain	Strain Rate	Time(sec)
1	0.0	.004	9.991E-5	40
2	.004	.006	4.784E-4	4
3	.006	.008	9.762E-4	2
4	.008	0	-5.0E-3	1.6
5	0	0	0.0	60
6	0	-.004	-9.878E-4	4
7	-.004	-.009	-9.795E-5	50
8	-.009	.006	9.933E-4	15
9	.006	008	9.532E-6	200
10	.008	.01	5.0E-3	.4
11	.01	.01	0	60
12	.01	.015	4.95E-4	10
13	.015	0	-1.4925E-3	15

The Walker model follows the shape of the stress strain curve better than the other models. This could be a result of the better modelling of the back stress growth and the lack of an inelastic strain rate exponent. The model of Krieg, et al. had n = 15.0 and Schmidt and Miller had n = 7.0. The constant values of work hardening have also been reported as reasons for this [3,21]. Bodner's model may be suffering from the lack of a back stress or the effects of the plastic work measure of strain hardening. However, further study would be required to show this. The corrected model of Krieg, et al. reproduces the actual stress levels best after initial yield. No explanation can be given for this at this time.

CONCLUSIONS AND RECOMMENDATIONS

Conclusions and Recommendations based on the Models

The theories of Walker and Bodner with exponentially based inelastic strain rate equations and dynamic recovery terms handle the strain rate sensitivity the best. Bodner's model shows less sensitivity to strain rate

jumps possibly due to the plastic work rate measure of strain hardening. The reproduction of the general shape using Walker's model may be aided by better modelling of the back stress term and by the exponentially based inelastic strain rate equation. The drag stress growth law of the Walker model provided the closest fit to data over several cycles at higher strain rates. The second cycle peak seen at the lower strain rates was modelled only by Walker. Bodner's model handled cyclic response best over several cycles at the lower strain rates due to the thermal recovery term. The solute strengthening correction caused numerical instability, negating the effect of thermal recovery during hold times and may have lessened the sensitivity to strain rate jumps.

Future study of these models could take two directions. First, a comparison to a material which does not exhibit strain ageing effects would be beneficial. The corrections necessary to account for this phenomenon masked some of the information which could have been obtained in this work. An example of this is information about the effect of strain jumps on the predictive capabilities of the models. The thermal recovery capabilities of the models were also adversely affected by the strain ageing corrections. The methods for calculating constants should be checked with a positive strain rate sensitive material.

Second, further study which concentrates on the specific model form should be carried out by the use of extended models. These would be models extended from the existing ones. An example of this would be to replace the inelastic strain measure of work hardening in the model of Krieg, et al. with a measure based on plastic work. The inelastic work measure in Bodner's model could be replaced with an inelastic strain measure. The extended models could then provide true insight into the ramifications of using a measure of plastic work. The effect of using an inelastic strain rate equation based on

exponential, power law, and hyperbolic sine functions could be studied. The advantages and disadvantages of providing a model with a back stress term could be studied by providing the Bodner model with one as Moreno and Jordan have done [22].

Conclusions and Recommendations based on the Calculation of Constants

The initial assumptions that back stress is responsible for hardening in monotonic tension and drag stress is responsible for cyclic hardening/softening appear to be good assumptions for this material system. These assumptions were used for every model in the hand calculations and the computer iterations with success. Krempl, McMahon, and Yao report that a changing drag stress parameter alters the strain rate sensitivity of the model [23]. This effect was not considered in this work and might warrant further study. The initial assumptions that thermal recovery is negligible for rapid tests ($\dot{\varepsilon} > 1.0X10^{-14}$ sec^{-1}), drag stress recovery dominates in low strain rate cyclic tests, and back stress recovery dominates in creep tests appear difficult to apply in the presence of solute strengthening effects. This material system requires that a correction for solute strengthening be employed before recovery effects can be calculated. The recovery effects were much smaller than the original hand calculations for the models of Krieg, et al., Bodner, and Walker produced. This observation leads to the conclusion that the recovery effects are largely insignificant for $\dot{\varepsilon} > 1.0X10^{-5}$ sec^{-1}. Miller's model requires the recovery terms to be much more active than the other models. This inflexibility gave some problems in the calculation of Miller's constants.

The solute strengthening effects also masked the true strain rate sensitivity of the material. Information on the strain rate sensitivity needs to be obtained outside the region of solute strengthening effects. The following initial assumptions would have been more appropriate based on these

observations:

(1) back stress was assumed responsible for hardening in monotonic tension;

(2) drag stress was assumed responsible for cyclic softening;

(3) thermal recovery effects were small and masked by solute strengthening effects;

(4) solute strengthening or strain aging effects masked the basic positive strain rate sensitivity of the material.

The model of Krieg et, al. was an easy model to work with since each term in the growth laws could be scaled somewhat separately of the others. An interesting observation of this model was that the constants of the inelastic strain rate equation could be swept over a broad range but the monotonic hardening remained relatively constant. There was also a mathematical ambiguity between the constant C and the scaling of the drag stress. The scaling could be transferred from one parameter to the other without any visible change in model response.

Bodner's model "converged" to the final constants with fewer iterations than the other models using the iterative scheme developed in this work. This was probably due to the lack of a back stress parameter. A mathematical ambiguity existed between n and the scaling of the internal state variables when information was not available to calculate n. This is why a value for n can often be picked and still produce a workable model.

Miller's model was highly coupled in that the recovery terms were not separated from the hardening terms. The recovery terms can therefore change the same order of magnitude as the hardening terms. Miller readily admits that this model is designed for materials which have a very active drag stress parameter [9]. He states that this model may not be applicable for this type of material system. However, a reevaluation of the constants for Miller's

model might prove fruitful. A majority of the constants should be calculated outside the region of solute strengthening effects and without artificially separating the hardening and recovery terms. A solute strengthening parameter would then be added to fit the response to the negative strain rate sensitive region.

Miller's model also maintains control over the saturated states of the internal state variables B and D with the A_1 and A_2 constants. A correction for strain ageing as well as cyclic work softening might be possible by controlling these saturated states. A recommendation for further study based on this model would contain an expanded study of back stress magnitudes over the entire strain rate region considered. A possible method for this is disscussed in reference 11. The latest form of Miller's model [24] should also be studied, as it may be used with material systems similar to this.

Walker's model holds promise for automating the calculation procedure for this type of material. Walker's model has fewer constants, appears to be tailored for this type of material, and can utilize the theta plot concept [2]. The drag stress scaling performs the same strain rate sensitivity functions as the n in the power law related models. Expanding knowledge of the back stress values would also be useful for this model.

Conclusions and Recommendations Based on the Experimental Work

The back stress measuring tests both in creep and in cyclic loading were very subjective and uncertain. However, their extreme usefulness and relative success in application with an automated test set-up warrant further study. It appears possible that these tests can be developed into useful inputs to the constant calculation process. More sensitive data acquisition devises with greater resolution and a smaller and less massive load frame for more precise control would greatly enhance the usefulness of these tests. The subjectivity could be lessened by using a method such as proposed by Blum and

Finkel [14] to analyze the data.

The back stress measuring tests during creep were useful for strain rates less than $1.0X10^{-7}$ sec^{-1}. The cyclic back stress measuring tests were useful for strain rates greater than $1.0X10^{-4}$ sec^{-1}. The region between these two tests could be filled by performing tests during monotonic tension such as the stress transient test mentioned by Soloman, Alhquist and Nix [16]. This type of test takes on greater usefulness for a material such as Inconel 718 which exhibits good ductility in tension and high susceptibility to low cycle fatigue.

An automated load frame was invaluable in this work for the complex tests. A smaller load frame might provide more stability during highly sensitive and mode-switching tests. A dead weight load frame would also be useful for the creep and creep-stress drop tests. A more advanced and controllable method of load-up would be a necessity. It would also be useful to utilize the same grips, furnace, extensometer, and data aquisition equipment as with the automated load frame. This would remove some relative errors between the two systems.

REFERENCES

1. Metals Handbook,9th edition, Volume 4 Heat Treating, American Society for Metals, Metals Park, Ohio.
2. U. S. Lindholm, K. S. Chan, S. R. Bodner, R. M. Weber, K. P. Walker, and B. N. Cassenti, Constitutive modelling for isotropic materials (HOST), Second annual contract report, NASA CR-174980 (1985).
3. R. D. Krieg, J. C. Swearengen, and R. W. Rhode, A physically-based internal variable model for rate-dependent plasticity. Proc. ASME/CSME PVP Conference, 15-27 (1978).
4. C. G. Schmidt, A Unified Phenomenological Model for Solute Hardening, Strain Hardening, and Their Interations in Type 316 Stainless Steel, Ph. D. Dissertation, Stanford University, Department of Materials Science and Engineering, (1979).
5. P. K. Imbrie, W. E. Haisler, and D. H. Allen, Evaluation of the numerical stability and sensitivity to material parameter variations for several unified constitutive models. MM 4998-85-61, Texas A&M University, (1985).
6. S. R. Bodner, Evolution equations for anisotropic hardening and damage of elastic-viscoplastic materials. Plasticity Today: Modelling, Methods, and Applications, Elsevier Applied Science Pub., Barking, England, (1984).
7. S. R. Bodner, Review of a unified elastic-viscoplastic theory. AFOSR-84-0042, (1984).
8. J. Friedel, Dislocations, Addison Wesley, 277-279, (1967).
9. A. K. Miller, An inelastic constitutive model for monotonic, cyclic, and creep deformation. part I-equations development and analytical procedures, part II-application to type 304 stainless steel. J. Eng. Mat. Tech. 98H, 97-113 (1976).
10. K. P. Walker and D. A. Wilson, Creep crack growth predictions in INCO 718 using a continuum damage model. Pro-ceedings of the 2nd Symposium on Nonlinear Constitutive Relations for High Temperature Applications, Cleveland, Ohio, (1984).
11. G. H. James, An experimental comparison of several viscoplastic models at elevated temperature, M.S. thesis, Texas A&M University, (1986).
12. K. P. Walker, Representation of Hastelloy-X behavior at elevated temperature with a functional theory of viscoplasticity. ASME Pressure Vessels Conference, San Francisco, California, (1980).
13. W. B. Jones, R. W. Rhode, and J. C. Swearengen, Deformation modelling and the strain transient dip test. Mechanical Testing for Deformation Model Development, STP 765, ASTM, 102-118 (1982).
14. W. Blum and A. Finkel, Acta Met. 30, 1705 (1982).
15. J. R. Ellis and D. N. Robinson, Some advances in experimentation supporting development of viscoplastic constitutive models. Pro-ceedings of the 2nd Symposium on Nonlinear Constitutive Relations for High Temperature Applications, Cleveland, Ohio, (1984).
16 A. A. Soloman, C. N. Ahlquist, and W. D. Nix, The effect

of recovery on the measurement of mean internal stresses. Scripta Met., 4, 231, (1970).
17. K. P. Walker, Research and development program for nonlinear structural modelling with advanced time-temperature dependent constitutive relationships. CR-165533, NASA, (1981).
18. J. M. Beek, A comparison of current models for nonlinear rate-dependent material behavior of crystalline solids, M. S. Thesis, Texas A&M University, (1986).
19. D. C. Stouffer, A constitutive representation for In-100. AFWAL-TR-81-4039, Wright-Patterson AFB, (1981).
20. D. Yao and E. Krempl, Viscoplasticity theory based on overstress. The prediction of monotonic and cyclic proportional and nonproportional loading paths of an aluminum alloy, Int. J. of Plasticity, 1/3, (1985), pp. 259-274.
21. A. K. Miller, Modelling of cyclic plasticity: improvements in simulating normal and anomalous Bauschinger effects. J. Eng. Mat. Tech. 102, 215-220 (1980).
22. V. Moreno, and E. H. Jordan, Prediction of material thermomechanical response with a unified viscoplastic constitutive model. Pro. of the 26th Structures, Structural Dynamics, and Materials Conference, Orlando, Florida, (1985).
23. E. Krempl, J. J. McMahon, and D. Yao, Viscoplasticity based on overstress with a differential growth law for the equilibrium stress. Proc. of the 2nd Symposium on Nonlinear Constitutive Relations for High Temperature Applications, Cleveland, Ohio, (1984).
24. T. C. Lowe and A. K. Miller, Improved constitutive equations for modelling strain softening - part 1: conceptual development and part 2: predictions for aluminum, J. Eng. Mat. Tech., 106, 337-348 (1984).

ORIGINAL PAGE IS
OF POOR QUALITY

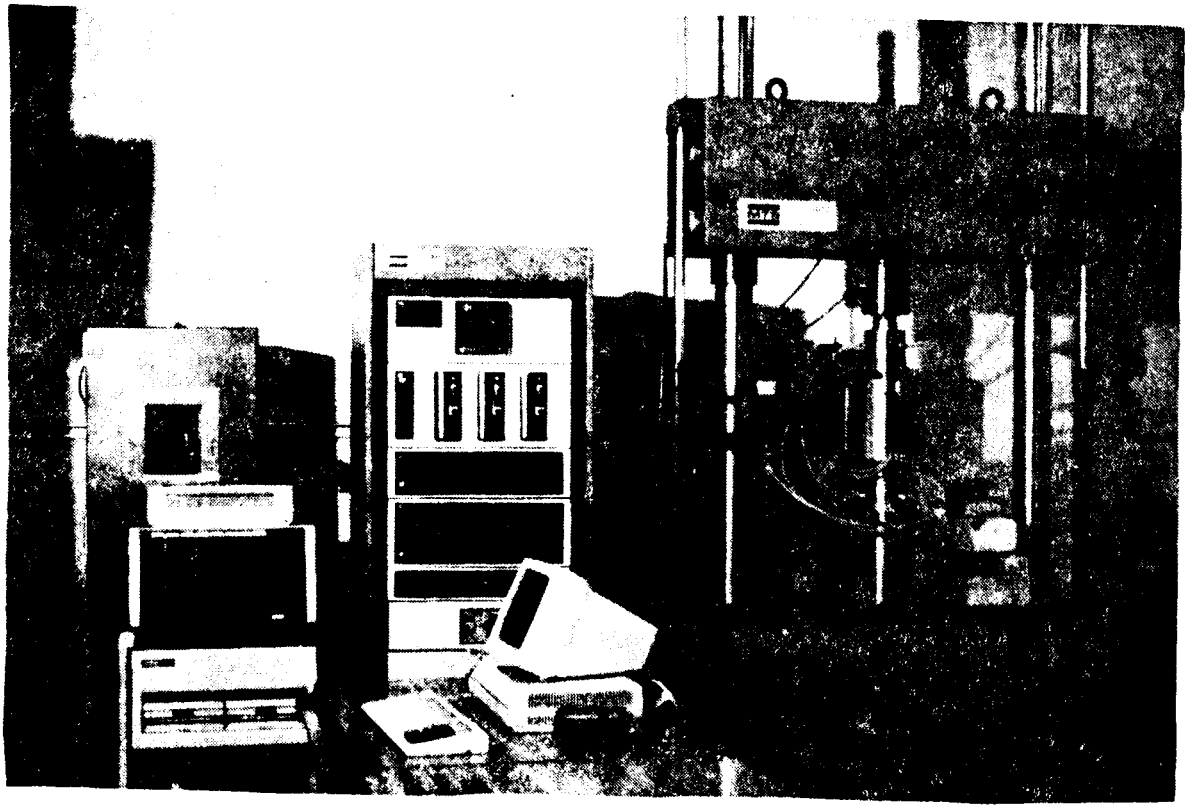

Fig. 1. MTS Configuration

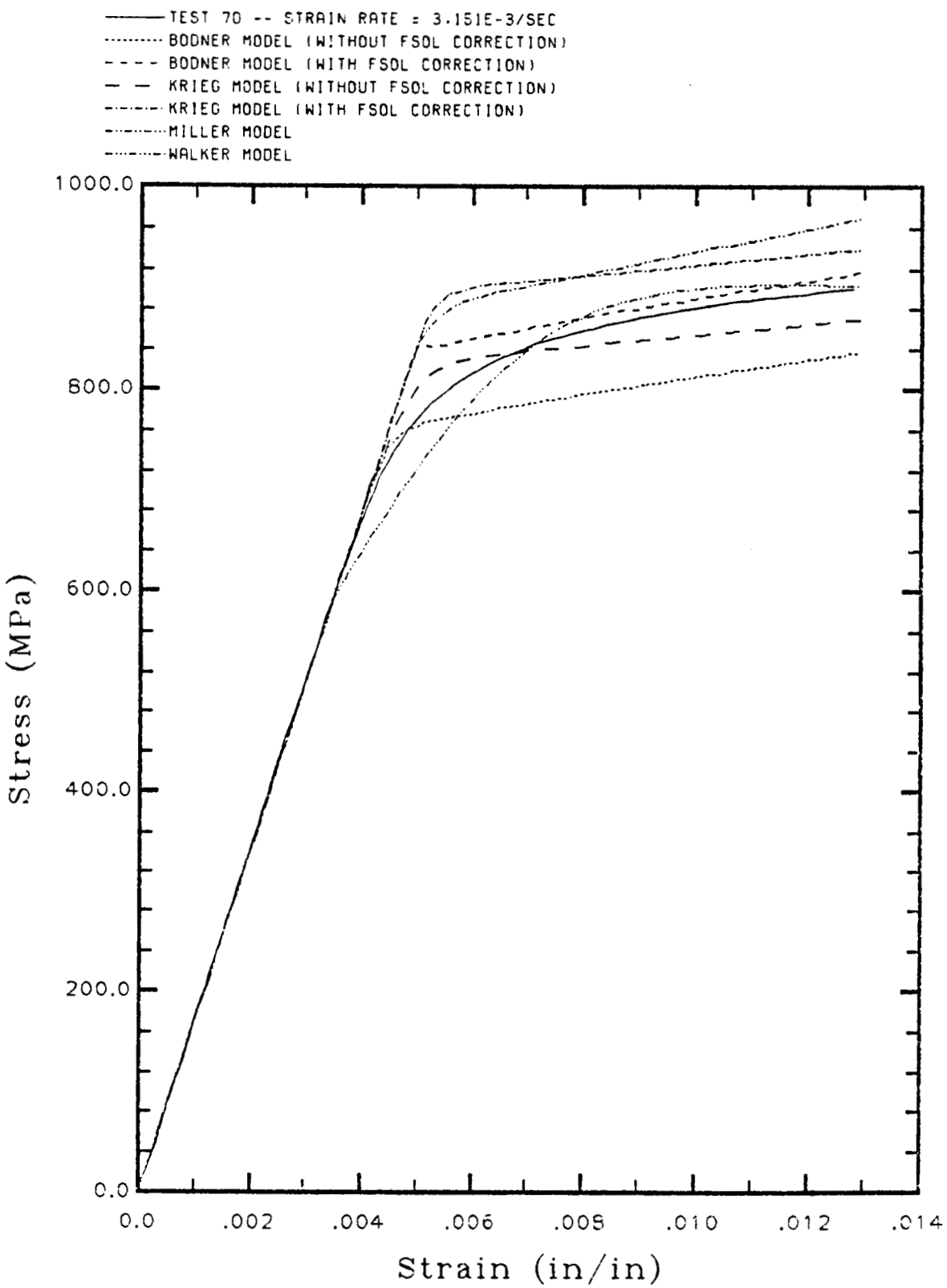

Fig. 2. Model Response as Compared to Test 70

C-4

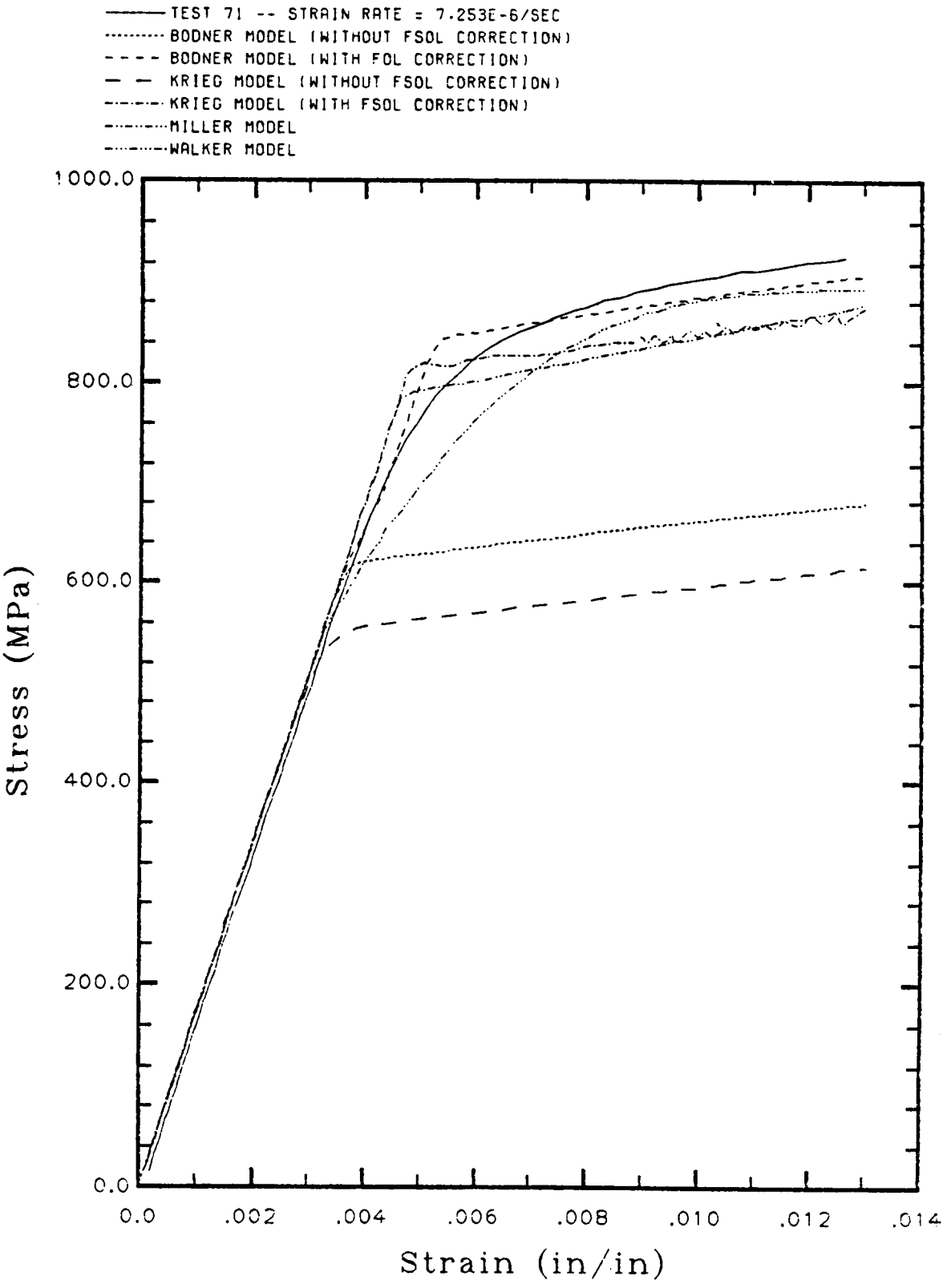

Fig. 3. Model Response as Compared to Test 71

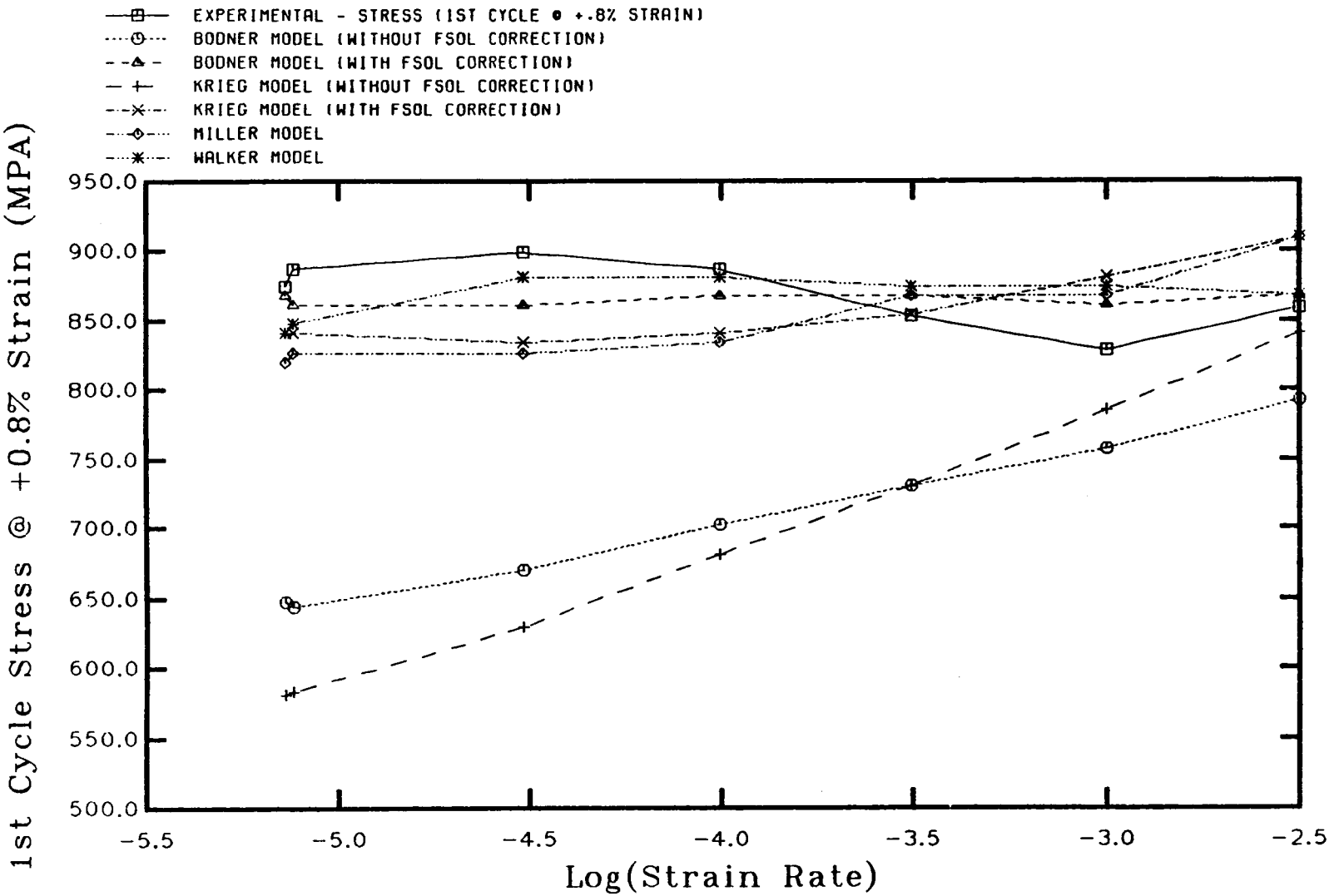

Fig. 4. Stress-Strain Response at +.8% for Cycle 1

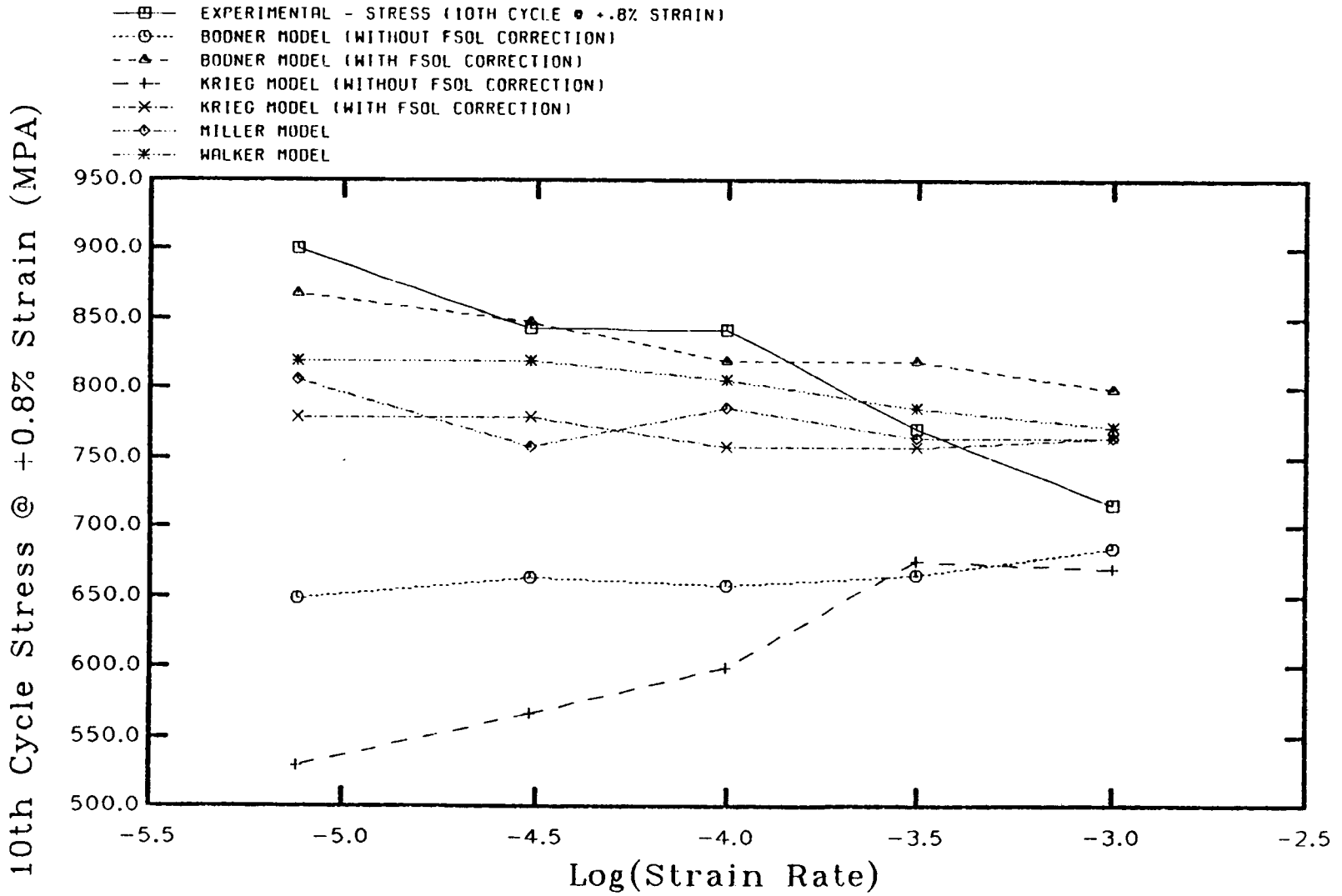

Fig. 5. Stress-Strain Response at +.8% Saturated Cycle

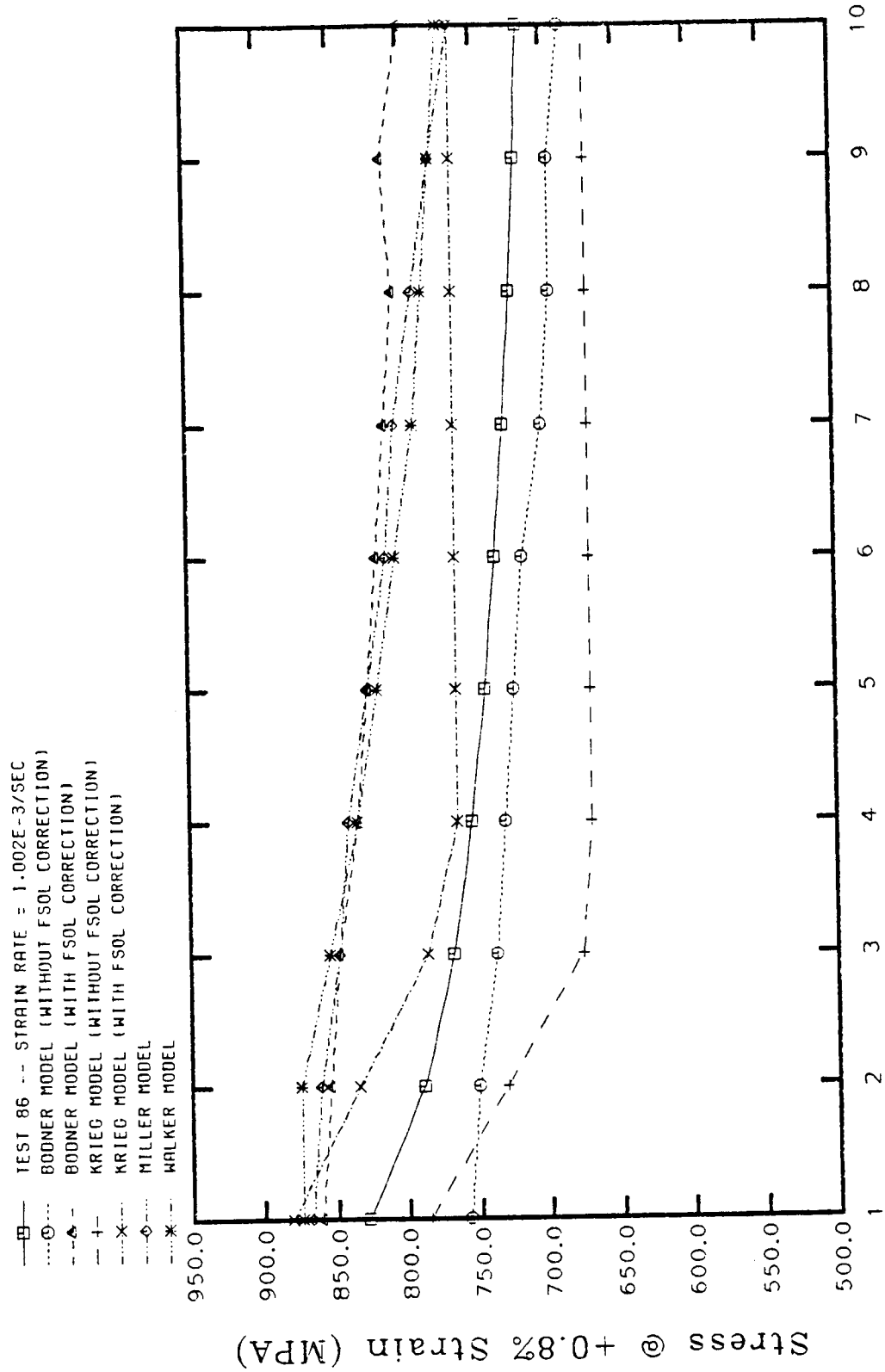

Fig. 6. Test 86 +.8% Response at Each Cycle

ORIGINAL PAGE IS
OE POOR QUALITY

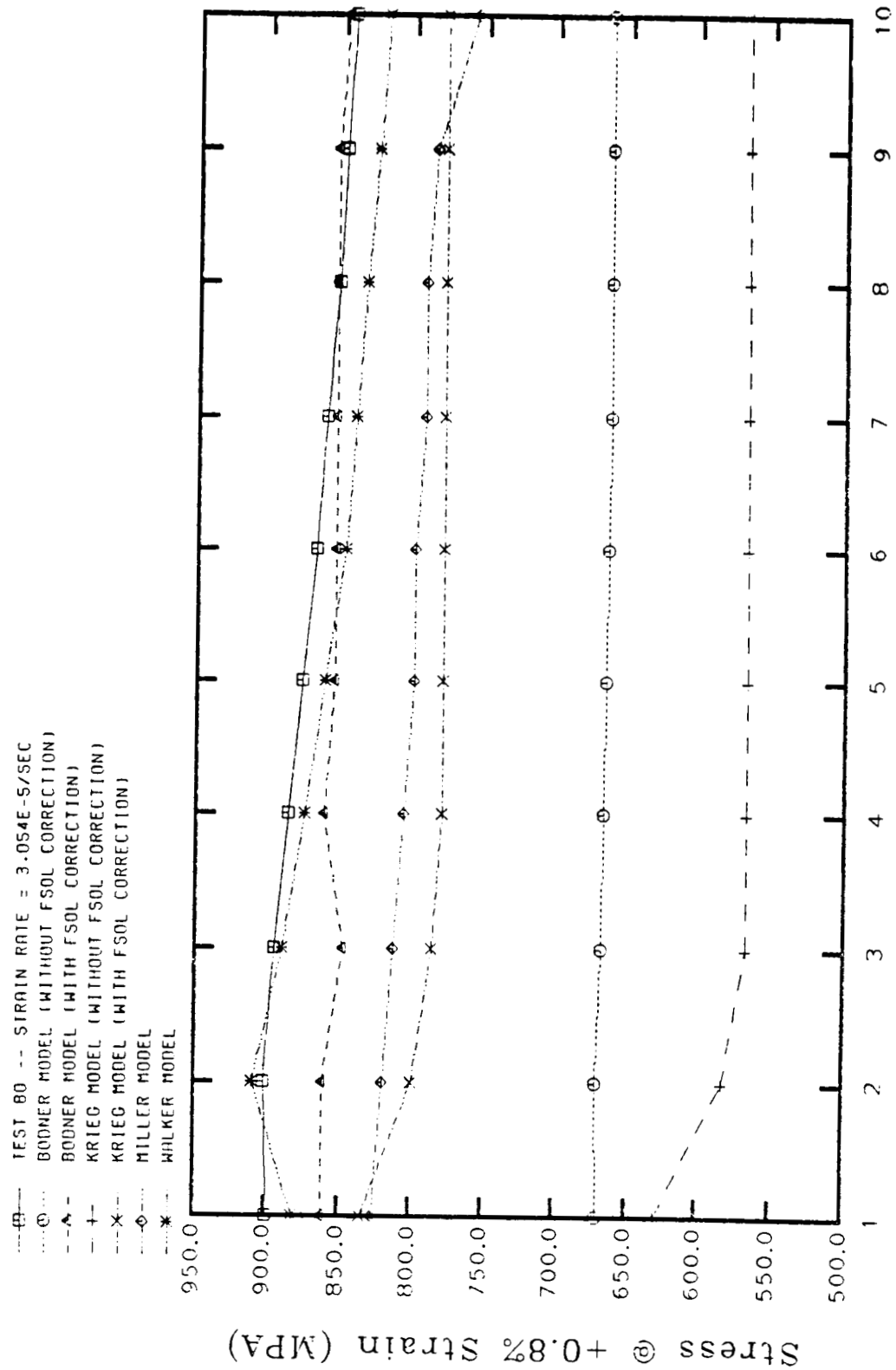

Fig. 7. Test 80 +.8% Response at Each Cycle

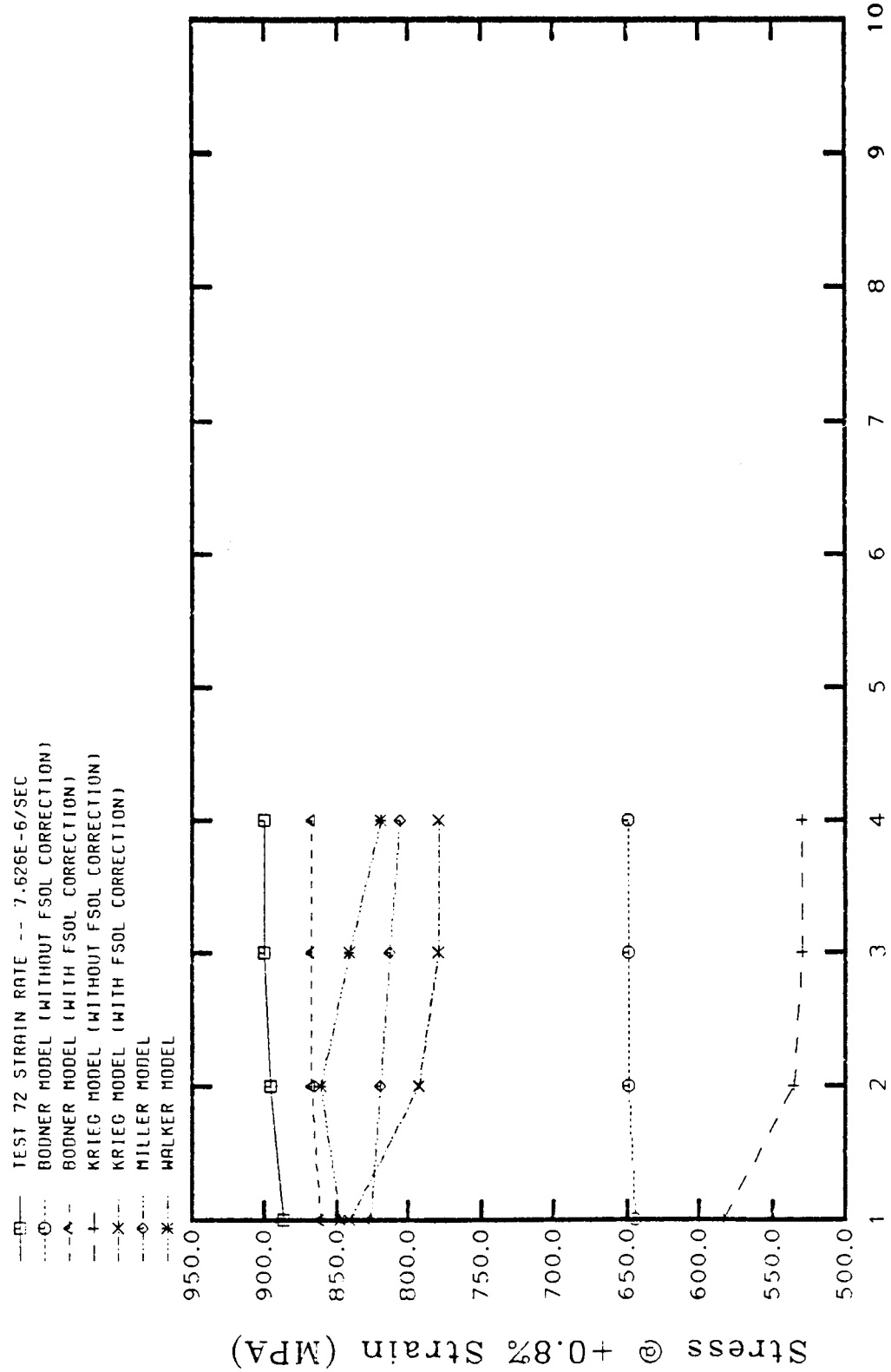

Fig. 8. Test 72 +.8% Response at Each Cycle

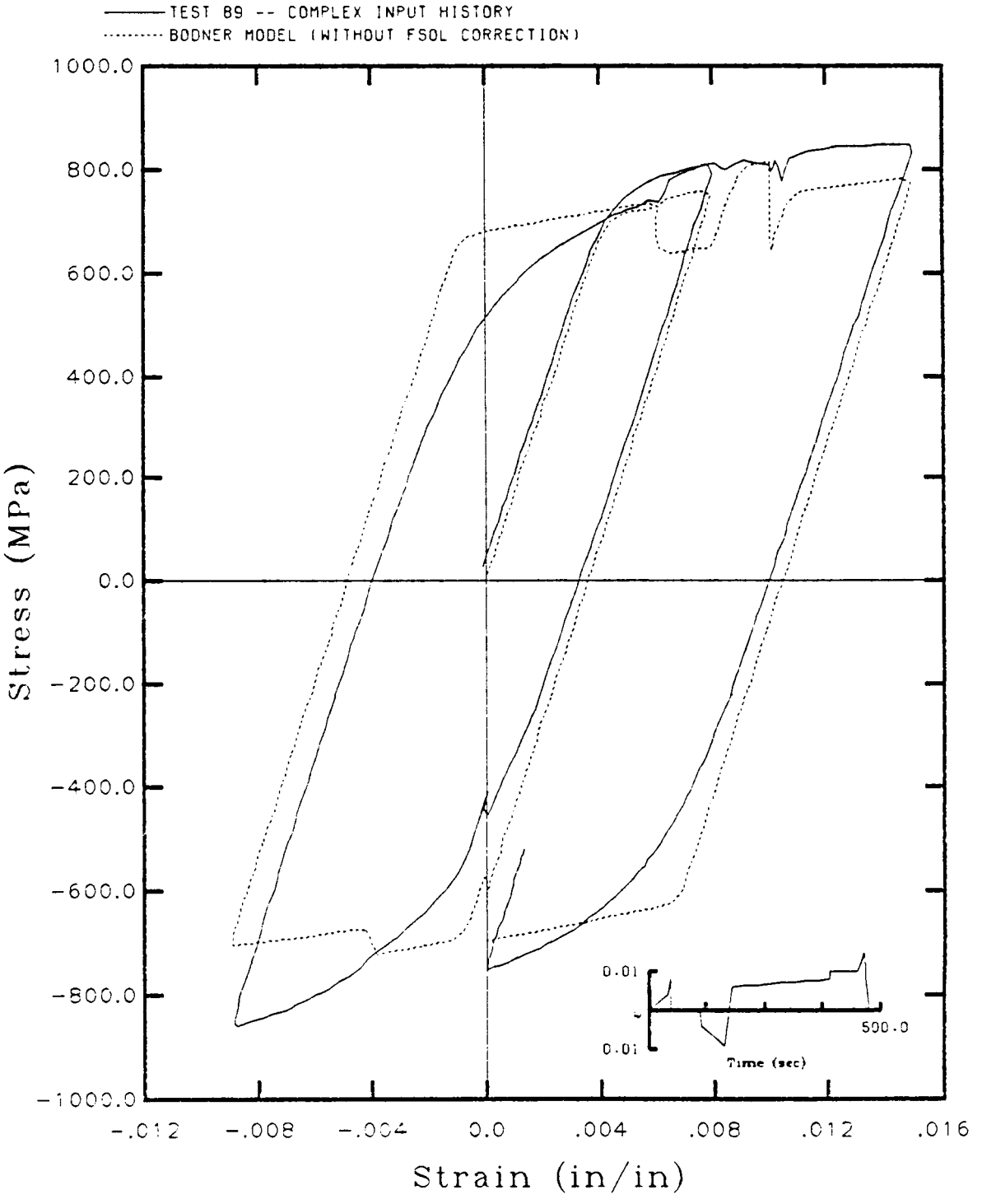

Fig. 9. Complex History - Bodner's Uncorrected Model

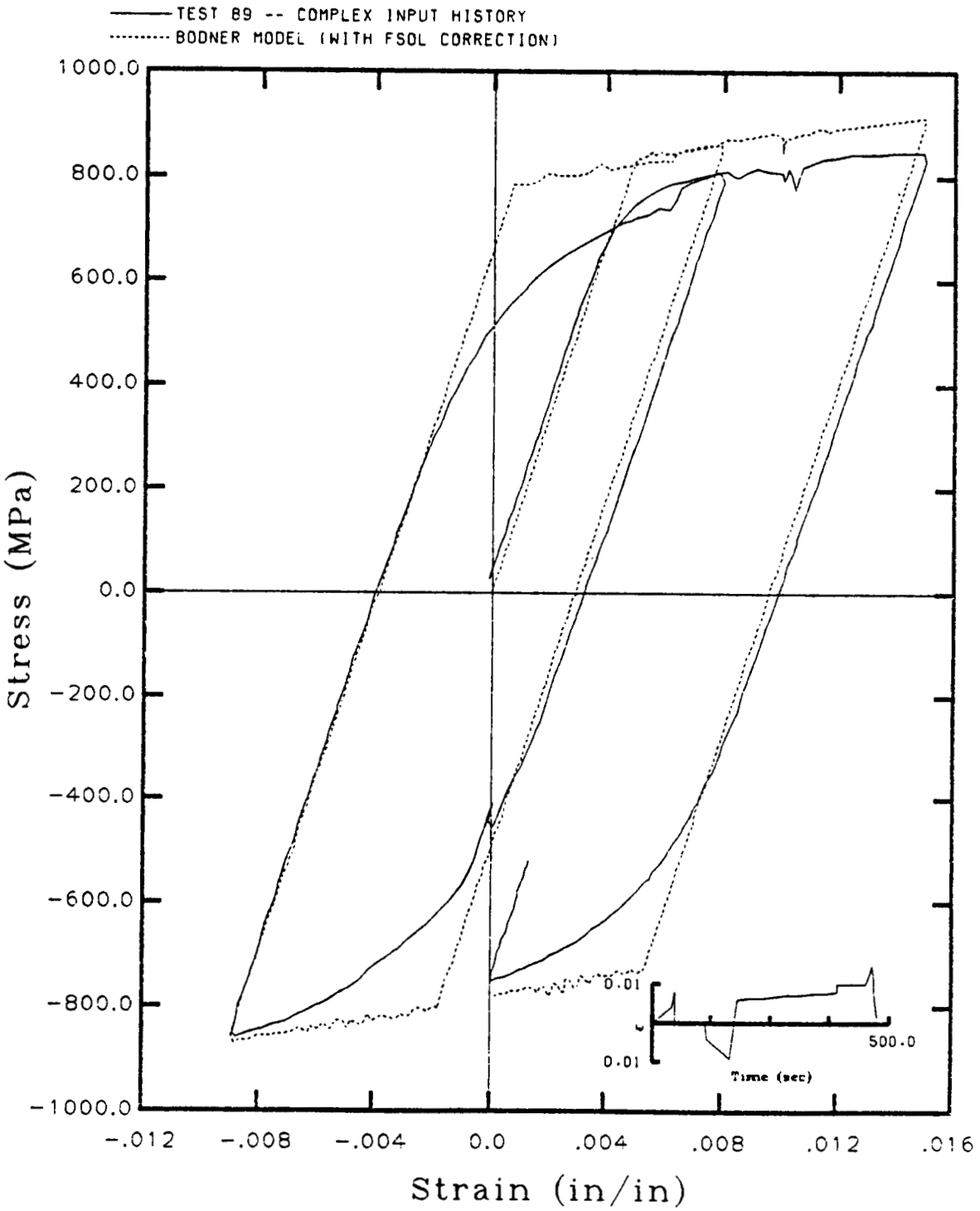

Fig. 10. Complex History - Bodner's Corrected Model

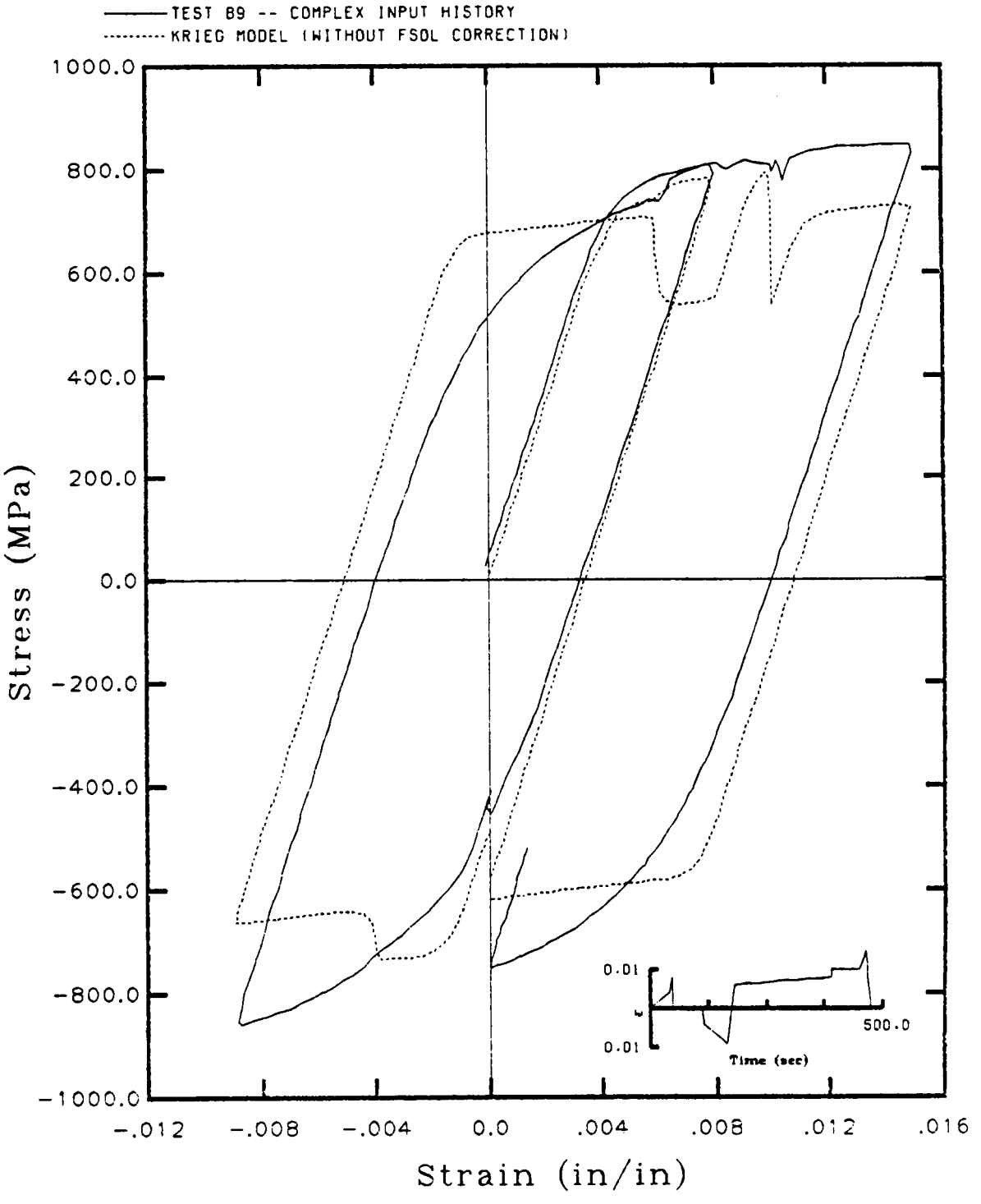

Fig. 11 Complex History - Uncorrected Model of Krieg, et al.

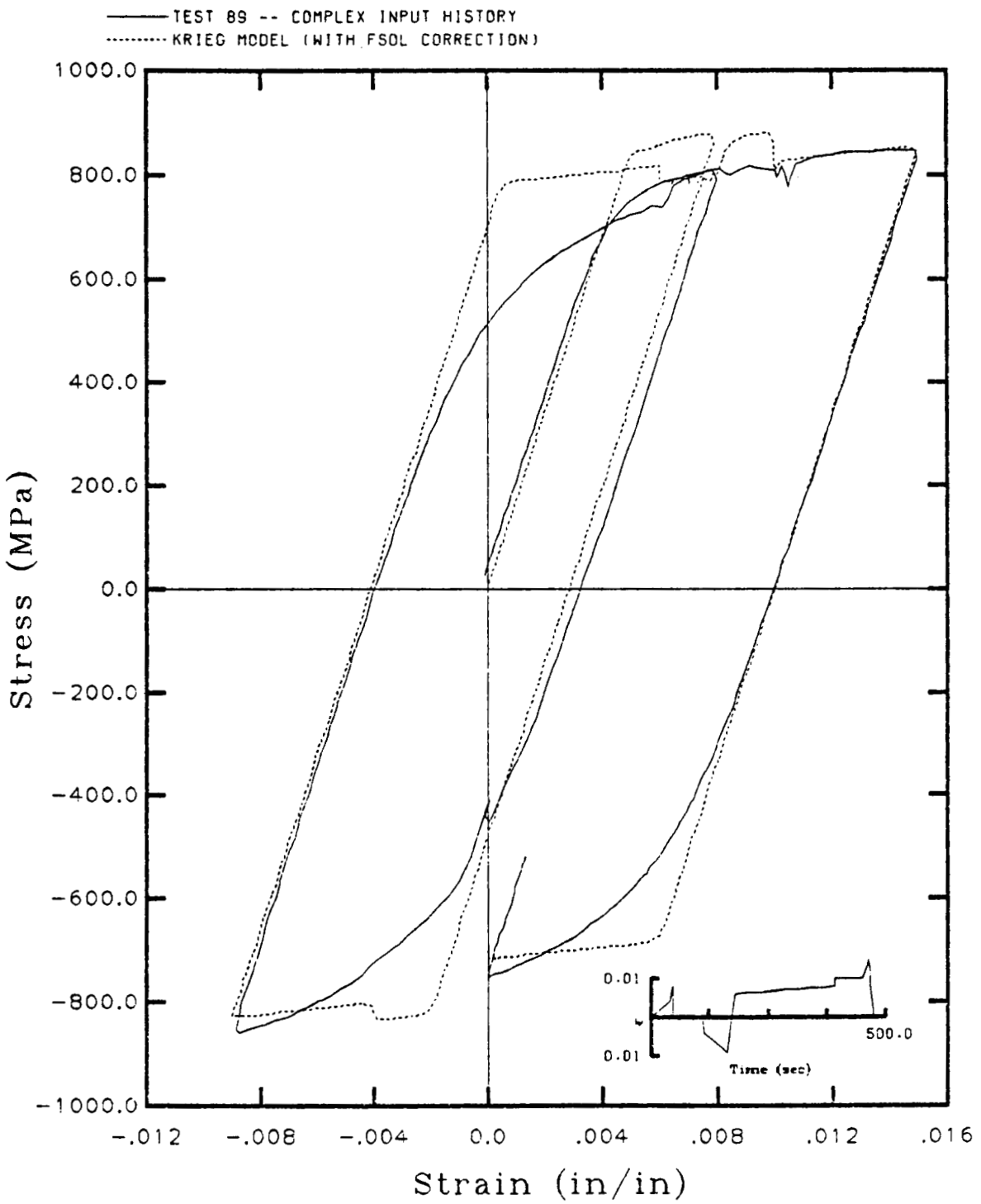

Fig. 12. Complex History - Corrected Model of Krieg, et al.

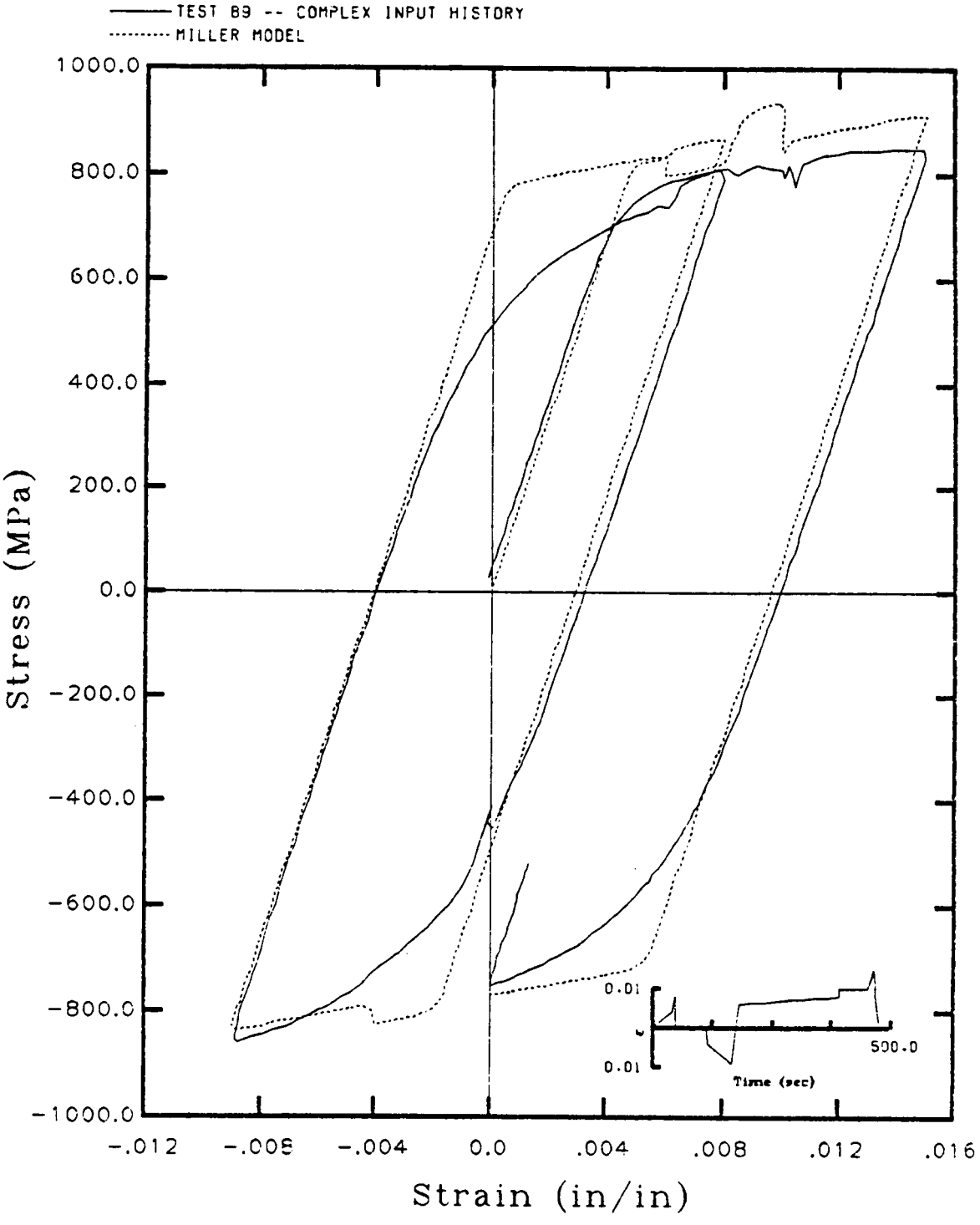

Fig. 13. Complex History - Schmidt and Miller's Model

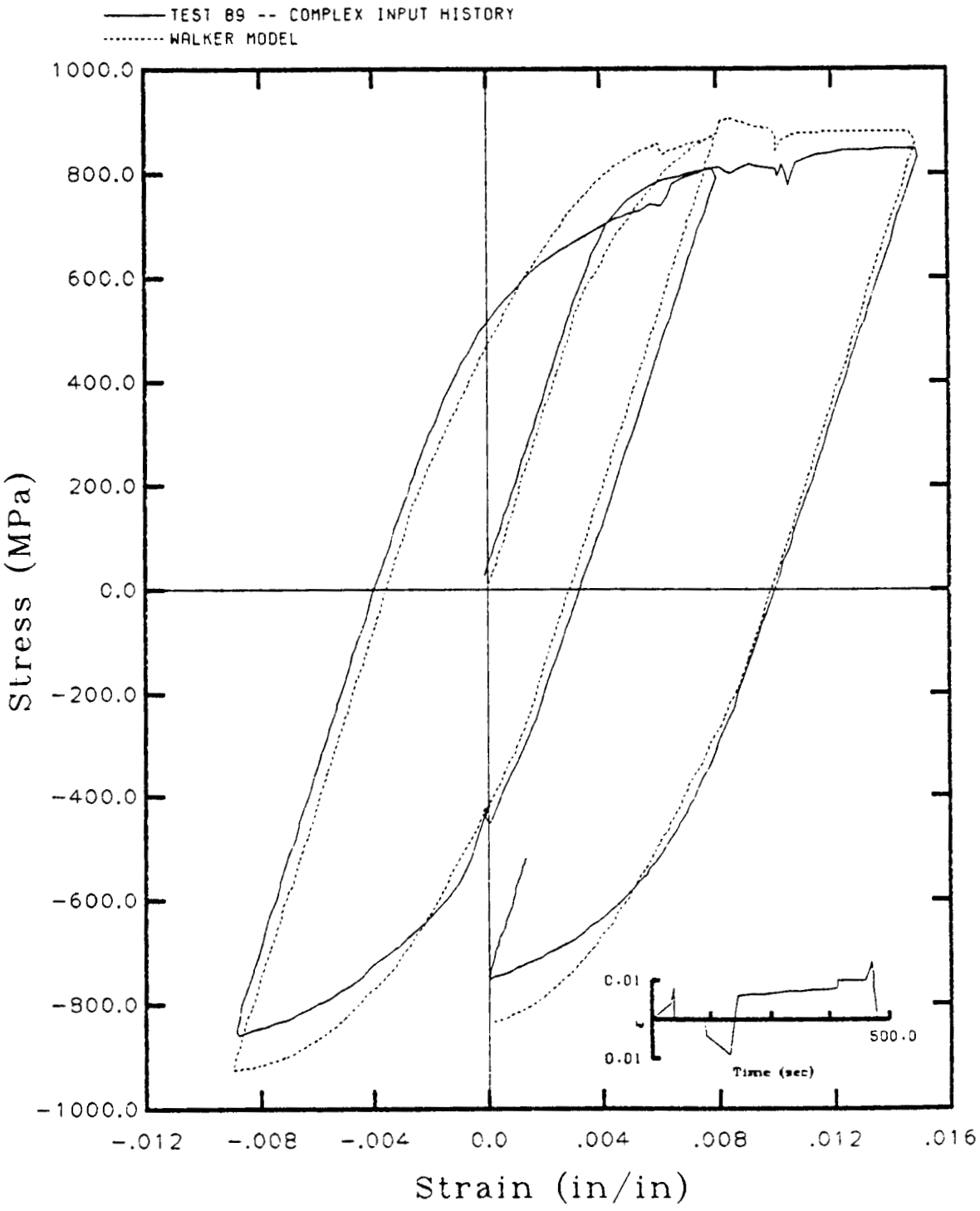

Fig. 14. Complex History - Walker's Model